

# **Investigating weathering signatures in terrestrial muds: Can climatic signatures be separated from provenance?**

Cansu Demirel-Floyd<sup>1</sup>, Gerilyn S. Soreghan<sup>1</sup>, Nina D.S. Webb<sup>2</sup>, Autumn Roche<sup>1</sup>, Young Ji Joo<sup>3</sup>, Brenda Hall<sup>4</sup>, Joseph S. Levy<sup>5</sup>, Andrew S. Elwood Madden<sup>1</sup>, and Megan E. Elwood Madden<sup>1</sup>

<sup>1</sup>School of Geosciences, University of Oklahoma, Norman, OK 73019, USA

<sup>2</sup>Impossible Sensing, St. Louis, MO 63118, USA

<sup>3</sup>Pukyong National University, Busan 48513, Republic of Korea

<sup>4</sup>School of Earth and Climate Sciences and Climate Change Institute, University of Maine, Orono, ME 04469, USA

<sup>5</sup>Department of Earth & Environmental Sciences, Colgate University, Hamilton, NY 13346, USA

**Data Availability Statement:** All data tables associated with this manuscript are available at U.S. Antarctic Program Data Center (USAP-DC) at <https://www.usap-dc.org/view/dataset/601599>.

## **SUPPLEMENTARY MATERIALS**

### **Supplementary Text**

#### **Detailed Geological Setting**

##### *Antarctica*

The McMurdo Dry Valleys (MDVs) are east-west trending icesheet-free valleys in Antarctica that are located between the Trans-Antarctic Mountains and the Ross Sea. With mean annual temperature (MAT) around -18°C (within -14°C to -30°C temperature range) and mean annual precipitation (MAP; mostly snowfall) of 100 mm/yr, the MDVs are considered as polar desert environments (Fountain et al., 1999; Doran et al., 2002, 2008). These valleys only contain active fluvial systems during 4-12 weeks of the austral summer, but host liquid water in ice-covered proglacial lakes year-round. Shallow permafrost layers hinder subsurface water flow, though there is shallow groundwater activity (McKnight et al., 1999; Gooseff et al., 2002, 2013) that is reported to be locally briny, which would allow water availability even through subzero winter conditions (Lyons et al., 1998; Lyons et al., 2005; Ball and Levy, 2015; Cuzzo et al., 2020; Lyons et al., 2021). Despite being an extremely cold and hyper-arid environment, chemical weathering still occurs within the austral summer within meltwaters, as inferred by solute fluxes in MDV meltwater streams (Gooseff et al., 2002; Stumpf et al., 2012; Lyons et al., 2015), and within rocks and soils (Guglielmin et al., 2005; Cuzzo et al., 2020).

Mechanical grinding of rocks/sediments under glaciers, as well as eolian redistribution of fine-grained glacial deposits supply fresh material available for weathering reactions (Stumpf et al., 2012; Marra et al., 2017). Though formerly thought to be a barren desert, now MDVs are known to house a diverse polyextremophilic microbial community within benthic lacustrine microbial mats, largely cyanobacterial mats in ephemeral streams, within endolithic

environments (soil and rock cracks), and in cryoconite holes (Cary et al., 2010; Cowan et al., 2010; Anesio and Laybourn-Parry, 2012). It is suggested that these communities are contributing to the nutrient fluxes within meltwater streams (i.e, Fe fluxes reaching to the Southern Ocean) via biological weathering, via in-situ microcosm studies and investigating the geochemistry of meltwaters (Maurice et al., 2002; Lyons et al., 2015). Photosynthetic microbial mats largely dominate the biogeochemical cycles, controlling C, N and P cycling (McKnight et al., 1999, 2004, 2007; Geyer et al., 2017; Smith et al., 2017), as well as providing nutrients via bioweathering of sediments with the help of heterotrophic organisms within MDV watersheds and soils (Demirel-Floyd et al., 2022).

We sampled glacial drifts, proglacial fluvial sediments, soils and water tracks within Wright Valley and Taylor Valley of MDVs, that were partially reported in previous publications (Hall et al., 1993; Hall et al., 2000; Marra et al., 2014, 2015, 2017; Levy et al., 2011). Drift deposits within the MDVs have different ages, composition, and texture due to complicated glacial histories, though both of the valleys are underlain by granitic and metamorphic bedrock (Hall et al., 1993; Hall et al. 2000, Hall and Denton, 2000; Hall and Denton, 2005; Hall, 2009; Hall et al. 2013).

### ***Taylor Valley***

Samples within Taylor Valley were collected from the Goldman Glacial Stream and deposits from Taylor Glacier predating 125 ka the Goldman Stream is flowing over, along with Ross Sea drift and Howard Glacier Stream sediments during the 2010 austral summer field season (Stumpf et al., 2012; Marra et al., 2014, 2015, 2017). We additionally collected soil

profile samples from one location, with 10 cm depth intervals, until reaching the permafrost at 40 cm. See Marra et al. (2017) for geology and sample location maps.

Eastern Taylor Valley deposits are largely affected by the encroachment of the Ross Sea Ice within the Taylor Valley, which introduced partially wet-based glacial conditions due to expansion of a grounded ice sheet in the Ross Embayment during Last Glacial Maximum (LGM; Hall et al., 2000). The drift deposits emplaced during this LGM glacial event within Taylor Valley are called Ross Sea drift, which also includes reworked marine sediments. Delta Stream (Hall et al., 2000), also referred as Howard Glacier Stream (Marra et al., 2017), flows on the Ross Sea drift deposits that contain clasts from the underlying granite and biotite orthogneiss, as well as kyanite, basalt, sandstone, and dolerite clasts that are sourced out of the valley (Hall et al., 2000). The western portion of the valley is covered by drifts from Taylor Glacier, an outlet of the East Antarctic Ice Sheet, that are also reworked by proglacial fluvial stream systems (Hall et al., 2000). These drifts also were produced by wet-based glacier conditions and exhibit a fine-grained matrix. Proglacial lakes, meltwater ponds and paleo-lake beds introduce salt to glacial deposits, as well as eolian sources and weathering processes (Bisson et al., 2005). Taylor Valley also hosts heterogeneous dry-frozen and shallow ice-cemented, poorly developed salty soils developing on late-Quaternary, Pliocene and Holocene-aged glacial drifts, marine sediments and paleo-lake beds (Campbell and Claridge, 2006; Bockheim and McLeod, 2008; Ugolini and Bockheim, 2008; Bockheim and McLeod, 2015). In austral summer, the upper 10-60 cm of the permafrost thaws, providing either a dry or melt-saturated active layer (Campbell et al., 1997; Bockheim et al., 2007). We refer to previous studies for further details about the drift deposits, soils and the glacial history of Taylor Valley (Hall et al. 2000; Hall and Denton, 2000; Higgins et al., 2000; Campbell and Claridge, 2006; Bockheim and McLeod, 2008).

### ***Water tracks***

Water track samples were collected in Taylor Valley, around Lake Hoare, Lake Fryxell, and Lake Bonney basins, sampled during a 2009-2010 field campaign and mapped by Levy et al. (2011). Water tracks are gully-like features that have darker toned surfaces, which are observed on gentle to steep slopes of soils with high moisture (Levy et al., 2008, 2011). Water track soils show the typical characteristics of sandy Antarctic soils with poorly developed profiles, but are generally saltier in composition, inferred by their electrical conductivity (Liu et al., 2002; Bockheim et al., 2008). Water tracks may be similar to those on Mars known as recurrent slope lineae, which are attributed to briny groundwater activity (Levy et al., 2011), which is potentially causing seasonal bright salt efflorescences on Taylor Valley soils (Liu et al., 2002). Besides their association with groundwater seeps, water tracks are also observed within dry ephemeral stream channels. Water tracks also contribute to proglacial lake nutrient budgets by transporting weathering solutes. Therefore, water tracks are considered to be the intermediate medium connecting hydrological cycles within Taylor Valley (Levy et al., 2011). See Levy et al. (2011) for further details about the water track sediments of Taylor Valley.

### ***Wright Valley***

Wright Valley sediments include multiple drift samples collected by Hall et al. (1993), and Onyx River, Denton Glacial Stream and Clark Glacial Stream samples collected during 2010 austral summer field campaign within the Wright Valley (Stumpf et al., 2012; Marra et al., 2014, 2015, 2017). We additionally collected soil samples from two soil profiles around Clark Glacier and upper Onyx River region, with 10 cm depth intervals, until reaching the permafrost at 30 cm. See Stumpf et al. (2012) and Marra et al. (2017) for geology and sampling maps.

The eastern end of the Wright Valley is underlain by a bedrock composition of granite, quartz monzonite and granodiorite (Brownworth and Denton plutons) and filled with pre-LGM drifts dating as old as Miocene that contain heterogeneously sample clasts from these bedrocks (Hall and Denton, 2005). Clark Glacier Stream (Marra et al., 2017) emanates from the Clark Glacier and drains into the Onyx River, flowing primarily over the Quaternary-aged Brownworth drift and potentially eroding clast from the underlying mid-Quaternary-aged Trilogy and Quaternary-aged Loke drifts. The Onyx River drains from Lake Brownworth and transects the whole valley, eroding additional sediment from Valkyrie, Loop, Peleus and various Alpine drifts. Poorly developed soils of Wright Valley are mainly located around the Wright Lower Glacier and Onyx River flood plains of, consisting of all of these drift deposits, as well as bedrocks clasts of Ferrar dolerite, Olympus granite gneiss, Vida granite, and microdiorite (Hall and Denton, 2005; Campbell and Claridge, 2006; Bockheim and McLeod, 2008). See previous studies for further details about the drift deposits, soils and the glacial history of Wright Valley (Hall et al., 1993; Hall and Denton, 2005; Campbell and Claridge, 2006; Bockheim and McLeod, 2008).

### ***Peru***

Our fluvial, glacial drift, and lacustrine samples were collected during January 2016 field season from two NE-SW trending proglacial valleys (Llanganuco and Paron) of the Cordillera Blanca Mountain range, that generally exhibit a cold and semi-arid climate regime with highly seasonal precipitation (MAT= 0-9°C; MAP= 800-1200 mm/yr), due to high elevation and El Niño– La Niña oscillations (Kaser et al., 1990, 2003; Vuille et al., 2008; Bury et al., 2011), despite its location near the equator. The hydrological cycle during the dry season (austral winter from June to September) consists of glacial streams and groundwater, and the water budget is reduced by sublimation processes (Vuille et al., 2008; Gordon et al. 2015). However, abundant

rainfall during austral summer (from October to May) may result in lake outburst events (Kaser, 2001). The wet season allows the western Cordillera Blanca glacial region to host meadows that are defined by swampy plains with grass, sedge, and wetland plants in high-moisture soils that are underlain by lacustrine sediments and glacial till (Kaser et al., 2003; Baraer et al., 2014; Gordon et al., 2015).

Cordillera Blanca is the region with the most glacier cover of the Peruvian Andes at high-elevation terrain, with peaks reaching up to 6768 m (Iturrizaga, 2014). Bedrock and sediment cover in Cordillera Blanca valleys are affected by the glacial history of the region, including substantial glacial retreat in the Little Ice Age (LIA) that exposed polished bedrock and formed proglacial lakes (Racoviteanu et al., 2008; Iturrizaga, 2014). Geomorphological landforms and the glacial sediment budget of the Cordillera Blanca valleys are additionally affected by erosion resulting from uplift and large earthquakes triggering catastrophic mass movements. Cordillera Blanca region is located within an active fault zone of the Callejon de Huaylas basin, that is largely normal faulted and designated by the Andean fold-thrust belt on the east. The Cordillera Blanca fault defines the boundary between Miocene aged granodioritic batholith and Mesozoic schist and sandstones, while cutting through the Rio Santa Valley Pleistocene moraines (Siame et al., 2006; Giovanni et al., 2010). A major mass movement triggered by an offshore subduction zone earthquake with the magnitude of 7.8 in 1970, filling up the glacial valleys and settlements with glacial muds and moraine deposits dramatically examples the effects of active tectonics on the Cordillera Blanca valley systems (Cluff 1971; Evans et al. 2009; Iturrizaga, 2008).

### ***Llanganuco Valley***

Llanganuco valley is largely underlain by the granodioritic and tonalitic Cordillera Blanca batholith and locally by pyrite and sulfide mineral-rich marine black shales of the Upper Jurassic Chicama formation, which is under ice cover (Wilson et al., 1995; Love et al., 2004).

Llanganuco valley slopes are susceptible to small and large-scale rockslides that feed the debris-dammed lakes (Iturrizaga, 2014). Llanganuco sediment budget was affected by a Huascaran debris avalanche, followed by the big Yungay mass movement event in 1970, majorly filling the Llanganuco Canyon and stopping at Ranrahirca village (Cluff, 1971). The debris thickness is reported to range between 10-40 ft locally, which contained massive boulders, gravel, mud ice and water, blocking the Llanganuco River and resulting in glacial lake level rises (Cluff 1971; Evans et al., 2009). We sampled fluvial sediments along the Llanganuco River throughout the Llanganuco Valley, extending down to Ranrahirca at the distal sampling point.

### ***Paron Valley***

Paron valley is a 15 km-long northern Cordillera Blanca glacial valley, extends towards the east of Caraz. Paron River draining through the Valley is a segment of the Lullan River catchment area that drains into the Pacific Ocean (Iturrizaga, 2018). The majority of the Paron valley is underlain by the Miocene batholith granodiorite complexes (Siame et al., 2006). Glacier-dammed lakes in this valley were suggested to be more frequent during LGM when glaciers were larger (Iturrizaga, 2018). We collected samples from the only remaining large glacier-dammed lake, Laguna Paron, as well as fluvial slackwater bar sediments from the Paron River throughout the Valley.

### ***Other Peruvian Sites***



We additionally carried out a sampling campaign on the NE of Huaraz, sampling glacial lake debris from the Llaka Lake (~14 km NE of Huaraz) and soil from Zona de Pitek (~7 km NE of Huaraz). The silty Llaka Lake debris contains modern drift deposits on granitic bedrock (with local metasediments) from a glacier bounded by 5000-6100 m high peaks (Vallunaraju, Ocshapalca, and Ranrapalca) of Toclaraju mountain. Soil samples of Zona da Pitek were collected 20 cm and 60 cm down the soil profile, at the road junction out of the same glacial valley where the Llaka Lake is located.

### *Norway*

Our glacial drift, soil, proglacial lake and fluvial sediment samples from Norway are collected from Austerdalen and Langedalen valleys of the the Jostedalsbreen glacial region during August-September 2014 field campaign (Joo et al., 2018b); the watersheds are underlain by mainly on quartz monzonite, granitic gneiss and granodiorite bedrock (Lutro and Tveten, 1996).

Josteldalsbreen ice cap is located between the east of the Nordfjord region and north of Sognefjord in the southwest cost of Norway, feeding S-NNW and N-S trending glacial valley streams draining into lakes and fjords. Nordfjord region is a part of Norwegian Caledonides, generally underlain by Precambrian acidic gneiss (granite to granodiorite composition) at the western section (Josteldalsbreen watershed) and dominated by basic pyroxene-granulite gneiss towards the east (Jotunheimen watershed; Mellor, 1987). The bedrock composition and structure are affected by Precambrian and Caledonian orogenies, as well as varying grades of metamorphism (Rye et al., 1997). The gneiss dominated bedrock has undergone ultrahigh and high-pressure metamorphism during continental subduction and is referred to generally as The Western Gneiss Region (Root et al., 2005; Butler et al., 2015).

Josteldalsbreen region has a cold and humid climate, determined by the MAT of 4.5° and MAP of 1769 mm/yr. The glaciomorphological sediment and landforms of the western Norway has imprints from the Little Ice Age (LIA) maxima of the late Holocene (Bickerton and Matthews, 1993; Lewis and Bernie, 2001). Non-glacial landforms were also changing during late LIA in the Josteldalsbreen area, recorded by a substantial increase in mass movements (Grove, 1972; Lewis and Bernie, 2001). Today, glacial valleys in the region are dominated by the fluvial fans, that hosts limited vegetation (grass, herbs, willows) in the active parts and well-developed scrubs and woodlands in the inactive sections (Innes, 1984).

### *Austerdalen Valley*

Austerdalsbreen foreland (elevation of 350 m) has MAT of 5°C and MAP of 2250 mm/yr (Green and Harding, 1980; Ostrem and Ziegler, 1969). The glacial meltwater stream in the Austerdalen valley joins with Langedalen valley proglacial stream and is named Storelvi river at the junction, which flows into the proglacial Veitastrond lake (King, 1959; Joo et al., 2022). We sampled fluvial sediment along a 16 km transect starting from the Austerdalen proglacial stream starting at glacier terminus and through the entire Storelvi river (~5 km segment), ending at the Veitastrond lake with a proglacial lake sample, as well as a distal and proximal glacial drift, and a soil profile (at 10, 20, 30, 50 and 100 cm depths) within the valley (Joo et al., 2018b, 2022).

Austerdalen Valley passes through a granitic basement (Lutro and Tveten, 1996), though we noticed that the valley is filled with banded gneiss and granitic gneiss boulders during our field observations (Soreghan et al., 2016; Joo et al., 2018b). The granite bedrock has contacts with monzonite at higher elevations of the glacier, migmatite towards the west in the Langedalen valley and a thrust phyllite at the SE of the Veitastrond lake (Lutro and Tveten, 1996).

Terminal and lateral moraines in Austerdalen valley contains glacial deposits that record the

glacial retreat after the maximum glacial advance in LIA. The Austerdalsbreen glacier is reported to have reached its maximum extent in recorded history in 1750, resulting in ten phases of moraine deposition (King, 1959).

### ***Langedalen Valley***

Langedalen valley is an approximately ~6 km-long valley trending from NW from the Langedalsbreen glacier to SE, joining the Austerdalen valley at the main channel of the Storelvi river. Langedalen valley is underlain by monzonite in the NE and approximately 20% of the transect is of granitic bedrock towards the valley exit on the SE (Lutro and Tveten, 1996). We sampled fluvial sediments approximately a ~4.5-km transect of the meltwater stream, starting at ~1.5 km distance from the source, and ending at the Austerdalen junction, as well as a proximal drift sample (Joo et al., 2018b).

### ***Iceland***

Iceland is a volcanic island in the South Atlantic Circle, underlain by volcanic rocks of 13 Ma-recent age and that has been experiencing silica-rich basaltic tephra ejections for the last 12,000 years (Andrews and Eberl, 2007). Climate isn't harsh due to the warm waters brought by the North Atlantic Current, though still cold with MAT ranging between 0-4°C, and humid with MAP >600 mm/year that supports vegetation (Olafsson et al., 2007). Low pressure regions commonly produce 5-15 m/s winds that can go up to 50 m/s during storm events; thus, aeolian processes contribute to landform evolution and sediment budgets of the fluvial catchments (Arnalds et al. 2016).

Icelandic glacial landforms are affected the late 19<sup>th</sup> century warming of the climate. Retreat of the Iceland ice caps exposed vegetated (largely birch) subglacial landscapes and

produced substantial dust, post glacial advance ~5000-4000 ago due to climatic shift (Hannesdottir et al., 2014; Arnalds et al. 2016). Glacial diamictons are formed through the erosion Tertiary and Quaternary volcanic sequences (Andrews and Helgadottir 2003). The Eyjafjallajökull volcanic eruption in 2010 (Sigmundsson et al. 2010) caused a catastrophic glacial outburst flood, which are common in the regions. These floods also contribute to the dust and sediment budgets as well as the landform development, as they rework former deposits and transport large amounts of fresh sediments (Prospero et al. 2012). Recharge of the Eyjafjallajökull volcano basaltic magma opened a short effusive fissure, potentially triggering the initial eruption of basaltic lava with SiO<sub>2</sub> content of 48% (Sigmundsson et al., 2010). Magma-ice interactions resulted in a secondary eruption within the ice-capped caldera of the volcano, resulting in a glacial outwash event (Sigmundsson et al., 2010).

We collected glacial outwash sediments from one of the S-N trending tributaries flowing over the Eyjafjallajökull glacial outwash deposits in a May 2016 field campaign. 3 fluvial sediment samples were collected from ~2 km segment of the glacial outwash tributary, starting ~1.3 km away from the source and ending at the junction to the river flowing on Katla glaciovolcanic outwash flood plains that drains into the ocean towards the SW.

### ***Washington***

We sampled fluvial sediments from Mountaineer Creek within Stuart Lake and Colchuck Lake catchment area at intervals until the junction with the Eightmile Creek at Mt. Stuart (at 3600-4800 m elevation), Washington State during A. June 2019 sampling campaign. We additionally sampled 2 glacial drifts (Mt. Stuart drift and Horseshoe Lake debris drift) on the slopes of Mt. Stuart (at 7200 and 5900 m elevation, respectively), as well as a topsoil on the lower banks of Mountaineer Creek.

Mt. Stuart is as a glaciated part of Washington Cascades that has a climate heavily affected by the topography, where high peaks act as a barrier for moist air masses (Reiners et al., 2003). MAP in the Northern Cascades region around Mt. Stuart is 1500-2000 mm/yr and MAT is ~8-10°C around Mt. Stuart (according to PRISM group 30-yr annual precipitation and temperature maps, Daly et al., 1994; Daly et al., 2008). Erosion rates across the Cascades are reported to show similar trends with precipitation profiles, reaching a maximum of 0.33 mm/yr, which is also associated with fluvial discharge (Reiners et al., 2003).

Our sampling site is located on the granitic bedrock of the Late Cretaceous calc-alkaline pluton that intruded the metamorphic basement (pre-Cretaceous Chiwaukum Schist) of the Cascades, which is called the Mt. Stuart Batholith (Erikson, 1977; Brown and Walker, 1993). Locally, lithology within the batholith might change between tonalite, quartz diorite, granodiorite, granite, gabbro, and ultramafite, and may be intruded by mafic Tertiary dikes. Mt. Stuart Batholith borderlines a NW trending horst, which is surrounded by the Deception-Straight Creek Fault, Leavenworth fault and Chiwaukum Graben (Erikson, 1977).

### ***Puerto Rico***

We collected fluvial sediment, saprolite and soil samples during May 2014 and 2018 from the Rio Guayanés and Rio Guayabo watersheds in southeastern Puerto Rico, which were heavily affected by Hurricane Maria in 2017 (Joo et al., 2018a, 2018b; Webb et al., 2022). These watersheds are largely underlain by Late Cretaceous San Lorenzo granodiorite, as well as quartz diorite, and minor metavolcanics (Rogers et al., 1979). The granodioritic bedrock hosts thick layers of soil and saprolite (up to 1m and 8m, respectively, Fletcher et al., 2006; Murphy et al., 2012). In a larger scale, the field site is within the Cordillera Central Mountain range, largely underlain by igneous rocks aged Jurassic to Eocene (Monroe, 1980). The region is also

tectonically active along the Puerto Rico Trench, which affects the landforms by 1 mm/yr uplift rates and moderate earthquakes (Mann et al., 2005).

Puerto Rico exhibits a hot and humid, tropical climate defined by MAT of 22°C and MAP of 4200 mm/yr (Joo et al., 2018a, 2018b). Puerto Rico is generally on the route of tropical storms and hurricanes, which are known to induce landslides (Lepore et al., 2012; Besette-Kirton et al., 2019). Increased deforestation due to anthropogenic activity additionally increases the susceptibility to landslides via destabilizing the water-saturated slopes (Larsen & Parks, 1997). Therefore, sediment budget within the watersheds is likely affected by anthropogenic erosion, chemical weathering, hurricane deposits, as well as storm induced landslides.

### ***Anza Borrego***

We collected fluvial sediment and soil samples from the Anza Borrego Desert, which is a 2400 km<sup>2</sup> section of the Sonoran Desert region, in December 2013. Anza Borrego has a hot and dry desert climate with MAT of 23°C and MAP of 150 mm/yr (Geiger & Pohl, 1953; Joo et al., 2016). There is limited fluvial transport within the watershed, but rare, intense precipitation events result in stream and overland flow (Joo et al., 2016; 2018b). This watershed is largely underlain by tonalitic bedrock, within a region that contains Jurassic metamorphic and Cretaceous plutonic units (Remeika & Lindsay, 1992).

Anza Borrego is largely affected by active tectonics due to activity along the Elsinore fault zones (Dorsey et al., 2011). Uplift of the Peninsular Ranges batholith may have been generating sediments via erosion since the Pliocene and early Pleistocene, forming Quaternary alluvial fans and filling up the “wineglass canyon”, where our study site is located (Remeika & Lindsay, 1992; Axen & Fletcher, 1998).

## Detailed Mineralogic Descriptions

### *Felsic minerals*

Quartz and feldspar combined compose the majority of all the mud-sized sediments examined, with feldspars being the most abundant phase (Table 3). Quartz + feldspar within most of the field sites are ~40-45%, except for significantly higher primary felsic mineral content in Peru (~83%) and Anza Borrego (~77%). The mud fractions with high felsic mineral content in Peru and Anza Borrego are composed of ~55% and ~60% feldspar and ~28% and ~16% quartz, respectively.

All field sites contain a range of calcic-sodic plagioclases and sodic-potassic alkali feldspars. Antarctica, Iceland, Norway and Puerto Rico are dominated by calcic plagioclases (labradorite>bytownite>anorthite), whereas Peru, Washington and Anza Borrego have higher sodic plagioclase content (albite dominated Washington and Anza Borrego; oligoclase dominated in Peru). K-feldspars (microcline and orthoclase) represent the alkali feldspar content in a majority of the sediments with occasional anorthoclase occurrences in Antarctic, Washington, and Peru samples. Plagioclase dominates the feldspar fraction in all field sites. Antarctica, Peru and Norway sediments have lower plagioclase/alkali feldspar ratios on average (2.7-3.5), compared to Anza Borrego, Puerto Rico and Washington sediments (8.3-9.3) that have significantly lower alkali feldspars abundances. Felsic mineral content of basaltic Iceland sediments, as they only contain 1.1% cristobalite and 0.6% alkali feldspar in average.

### *Mafic minerals*

Mafic primary mineral concentrations are significantly lower in the mud fractions from Peru (0.7%) and Norway (1.7%) sediments, whereas mafic mineral concentrations are highest in Iceland sediments (62.1%), as expected. Antarctica, Washington and Puerto Rico sediments have

similar mafic primary mineral contents on average (10%, 15%, and 11%, respectively).

Amongst the mafic minerals observed, mud-sized sediments from Iceland and Antarctica contain higher pyroxene contents, while amphibole dominates in Puerto Rico, Washington and Norway sediments, and Peru sediments contain almost equal concentrations of both. Anza Borrego sediments do not contain any mafic minerals (other than biotite) and Iceland sediments are the only samples containing olivine (forsterite).

Iceland sediments have the highest pyroxene content (18.6%), followed by Antarctic samples (6.7%). Other field sites contain less than 1% pyroxene on average with some local enrichments (Table 3). Overall, pyroxene compositions are dominated by clinopyroxenes (augite>diopside>hedenbergite). However, orthopyroxene (enstatite) also occurs in muds collected in Iceland and Wright Valley (Antarctica) in lower abundance.

Washington and Puerto Rico muds have higher amphibole contents on average (15% and 11%, respectively), followed by Antarctica (3.6%), Norway (1.7%) and Peru sediments (0.3%). Icelandic muds do not contain amphiboles. Actinolite dominates the amphibole content of most of the muds i, with tremolite content higher in Antarctic sediments and only hornblende observed in Puerto Rico muds. Occasional edenite (Antarctic Wright Valley, Washington), richterite (Peru) and ferri-clinoholmquistite (Washington) were also observed. Note that the Washington field area is partially underlain by bedrock that includes amphibolite facies accompanied by epidote occurrences, resulting in the highest diversity in amphibole content as compared to other field sites.

### ***Mica***

Overall, mica content is (muscovite + biotite + phlogopite; Table 3) is highest in Peru and Antarctica sediments (~11% on average), followed by Anza Borrego (8%), Washington



(6.1%), Puerto Rico (4.5%) and Norway (2.5%). Iceland muds do not contain any mica minerals. Puerto Rico mica content is exclusively biotite, which generally predominates in muds from all the other field sites except Norway. Norway muds contain muscovite, except for one drift sample with biotite. Muscovite was also observed commonly in Peru and Antarctic muds where it can locally dominate the mica content or is present in equal abundance to biotite. Phlogopite was also observed in Washington and Anza Borrego muds. It is also important to note that most of the Antarctic sampling locations are underlain by biotite orthogneiss (Hall et al., 2000; Marra et al., 2017), resulting in the higher biotite content of Antarctic sediments.

### ***Accessory minerals***

Accessory mineral phases are generally Fe- and Ti-oxides, as well as rare apatite occurrences observed the within muds from all field sites. Antarctic sediments also commonly contained cordierite group minerals which were not observed in the other sites. Abundances of accessory minerals are reported in Table 3 as the sum of all accessory minerals within each sample.

Antarctic muds contain birnessite (Taylor Valley), magnetite (Wright Valley), as well as apatite (Wright Valley). Iceland muds contain ilmenite and magnetite, whereas we detected hematite in only Norway soils, and Washington muds contain titanite and anatase as accessory oxides. Joo et al. (2018) reported up to 1.4% Fe-oxides in Anza Borrego muds, though we did not detect any in our analyses, potentially due to falling below detection limit of 1%.

Note that wet sieving and treating the muds with acetic acid and hydrogen peroxide like removed any salts, carbonates, and sulfide species, respectively. We also noted individual occurrences of apatite within Taylor Valley and Washington. However, these occurrences were modeled below 1% by the Jade software, therefore, we did not take them into account, using a

detection limit of 1%. However, apatite can dissolve with washing and acid treatments and could be more concentrated in higher grain sizes.

### ***Zeolites***

Zeolites were only observed within glacial settings, where the highest concentrations are observed within Washington muds (8.5% on average), followed by Norway (0.9%), Antarctica (0.7%), Iceland (0.7%), and Peru (0.2%). Washington sediments show the highest abundances of zeolites within the mud fraction, with laumontite concentrations reach up to 21% within glaciofluvial muds with rest of the zeolite composition generally consisting of stilbite and analcime. Zeolite concentrations within Norway muds reach up to 5%, mostly composed of heulandite and babingtonite. Though the average concentration of zeolite is low in Antarctic muds, zeolite occurrences are more frequent and diverse, ranging between 1-8.7%, where chabazite, babingtonite, heulandite and clinoptilolite. Iceland and Peru muds had only one detectable zeolite occurrence each, with 2% and 2.6% abundance, respectively.

### ***Amorphous phases***

Based on the XRD data, amorphous phases are likely common in both the Icelandic and Antarctic sediment samples. We infer from the hump-shaped background observed within the XRD pattern (Figure S1) is due to amorphous silica-rich phases. Therefore, we did further modeling analysis of the mineralogy observed within an Antarctic glacial drift (T10-HOW-9Drift) with ClaySIM to elucidate potential amorphous phases. Our analysis indicated that up to 7-8% of the clay-sized fraction was composed of amorphous smectite within the Antarctic drift. Total amorphous content within Icelandic sediments were comparable between Jade and ClaySIM (20-38%, Table 3). According to the representative ClaySIM modeling of Icelandic glacial outwash meltwater stream sample (EYF-2-IS), 4-8% of the amorphous phases are likely

amorphous smectites, with the rest being composed of volcanic glass. Jade analyses also included 2-4% Opal-A within the Icelandic amorphous phases. In Table 3, we report the total amorphous content (Opal-A + other amorphous silica) modeled by the Jade software.

## Supplementary Figures

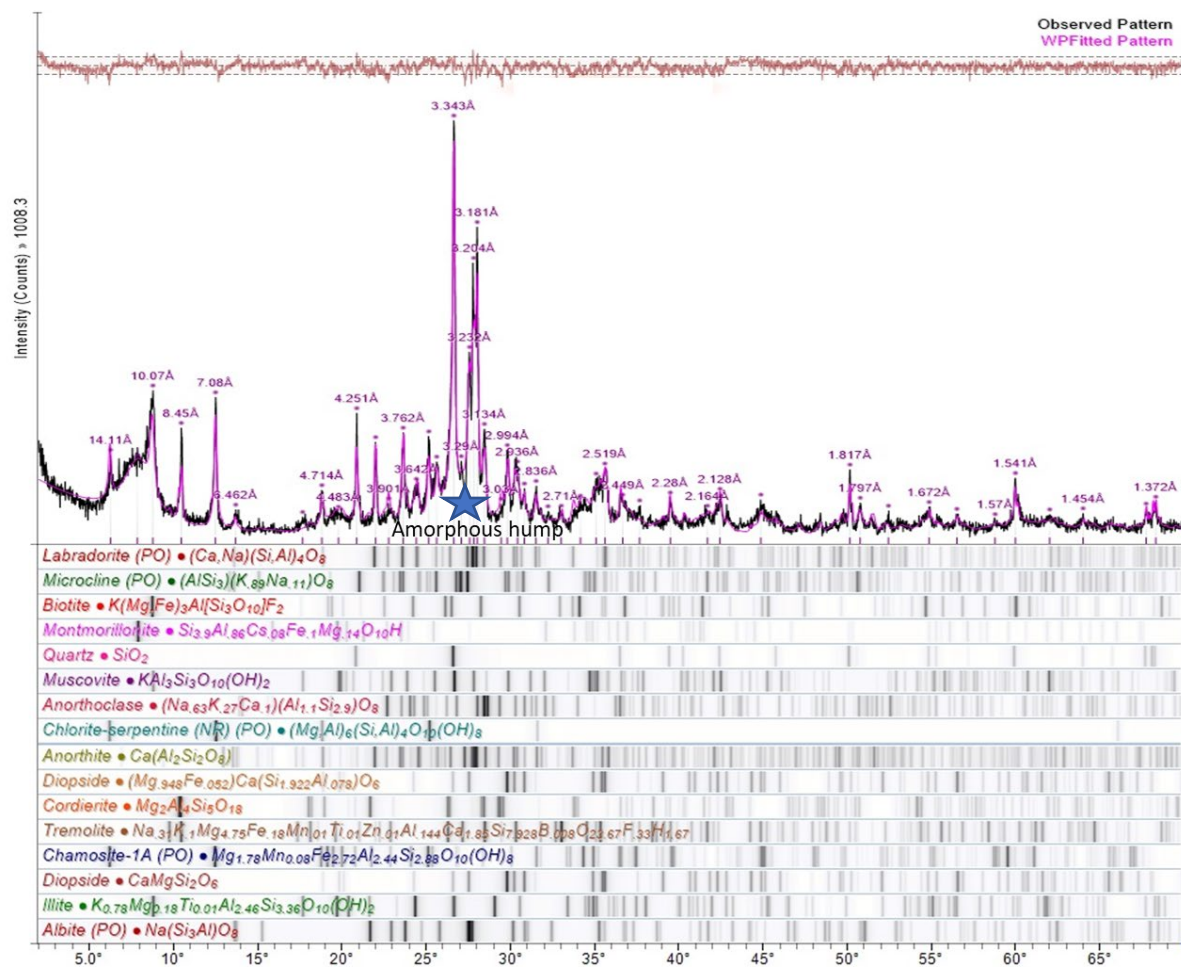


Figure S1. Example XRD pattern fitting with JADE software on an Antarctic Taylor Valley drift sample (T10-HOW-9Drift). Blue star demonstrates the location of the “amorphous hump” that shows there are amorphous phases in Antarctic samples.

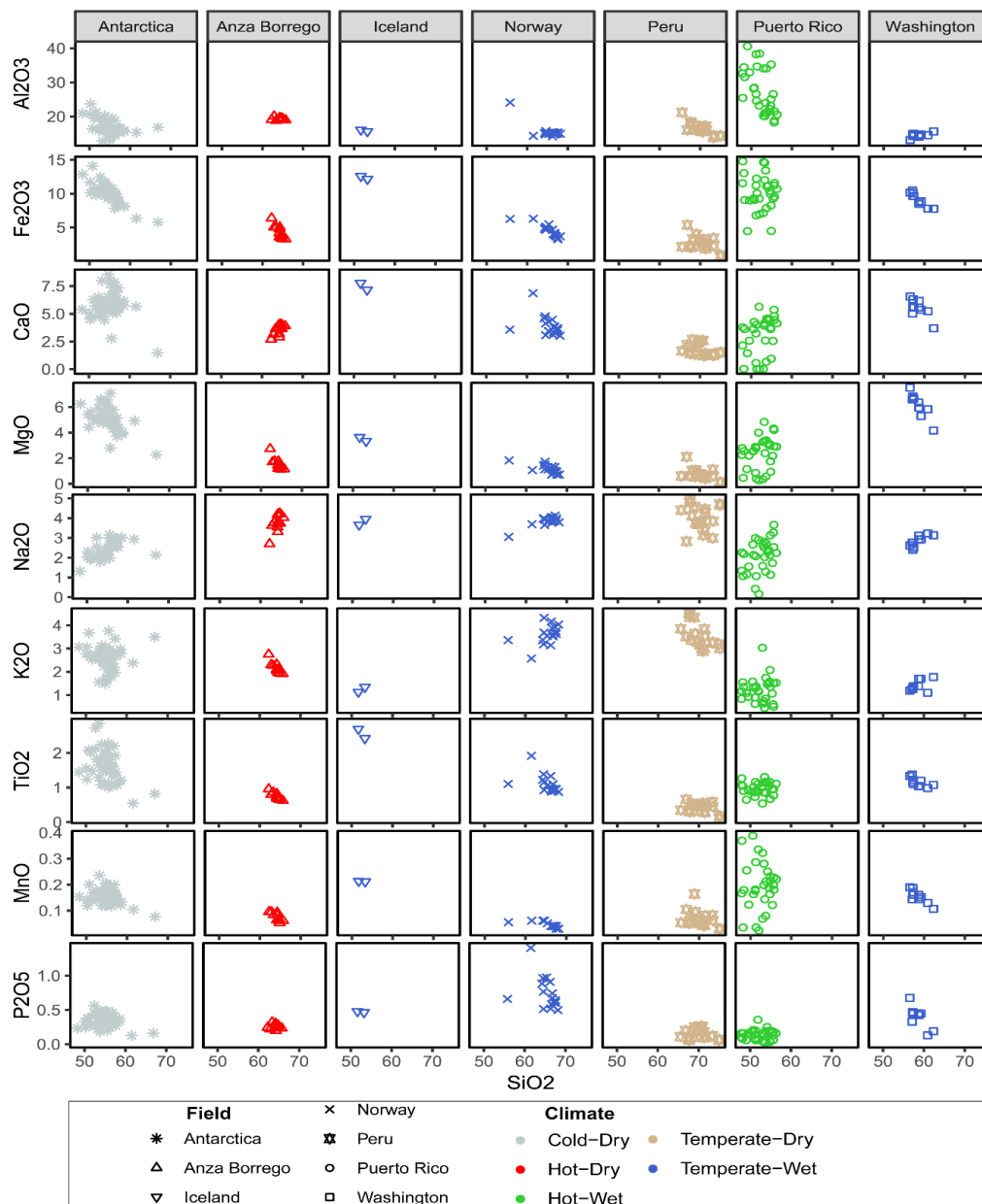


Figure S2. Selected major oxides plotted against  $\text{SiO}_2$  for all field sites. All concentrations are in wt %, and data points are colored with respect to climatic regime, as illustrated in the legend. The most obvious trends suggestive of weathering are the decreasing of  $\text{Al}_2\text{O}_3$  concentrations with increasing  $\text{SiO}_2$  within Antarctica, Peru, and Puerto Rico muds.